

Travel time estimation methods for mode tomography

Tarun K. Chandrayadula
George Mason University
Electrical and Computer Engineering Department
4400 University Drive, MSN 1G5
Fairfax, VA 22030
phone: (703) 993-1610 fax: (703) 993-1601 email: tchandra@gmu.edu

Award Number: N00014-06-1-0223

LONG-TERM GOALS

The long term goals of this project are to investigate statistical models for signals propagating in long-range underwater channels and to design signal processing techniques to mitigate signal fluctuations due to random disturbances such as internal waves.

OBJECTIVES

At long ranges, broadband receptions consist of early ray-like arrivals and a finale that is best described in terms of the low order modes. The energetic low mode signals are more strongly affected by internal wave scattering than the ray arrivals. By focusing on the low modes, this project seeks to develop a better understanding of internal wave effects. The first objective of this project is to derive range-dependent mode statistics from experimental data obtained during the SPICE04 and LOAPEX experiments. The second objective of this project is to develop new robust signal processing techniques to estimate the travel times of the modes based on the derived statistical channel model.

APPROACH

To characterize internal wave effects on the modes, this project used the extensive data sets of low-frequency receptions recorded as a part of the North Pacific Acoustic Laboratory (NPAL) project. Two specific experiments are particularly relevant for the current work. First, the Long Range Ocean Acoustic Propagation EXperiment (LOAPEX) conducted in 2004 provided a unique opportunity to measure low mode receptions at a series of ranges from 50 km to 3200 km. In addition to LOAPEX, the SPICE04 experiment included transmissions from a bottom-mounted source at Kauai to a receiving array at a range of 2400 km. This project analyzed the LOAPEX and Kauai receptions and has compared the results to Parabolic Equation (PE) simulations. The results of this analysis were used to develop random channel models for the low order modes and subsequently develop new signal processing techniques for these modes.

The principal investigator for this project is Tarun K. Chandrayadula, who received a Ph.D. from

George Mason University in January 2010. His thesis advisor is Professor Kathleen E. Wage.

WORK COMPLETED

Mode Tomography and Signal Processing: Perturbations to the mode excitation spectrum due to internal waves were analyzed using simulated data, and a model based on second-order statistics was constructed. Matched subspace detectors based on this statistical model were used to estimate the mode travel times at LOAPEX stations T50 and T250. The estimated travel times were used to invert for the range-averaged sound speed profile (SSP) along the LOAPEX path. The inverted profiles were consistent with point measurements made during the experiment. These results were presented at the North Pacific Acoustic Laboratory (NPAL) workshop in August 2009 and the ASA meeting in October 2009 [5]. Two journal articles are currently in preparation.

Internal Wave Simulations: Internal wave effects across a 400 km range were modeled by using the method suggested by Colosi and Brown [6]. In order to analyze mode propagation through internal waves, two types of simulations were implemented. First, coupled mode simulations were performed to calculate the amplitude and phase statistics of the unscattered mode signals. Second, parabolic equation (PE) simulations were used to estimate range-dependent statistics of the total mode signals (unscattered plus scattered). Results of this simulation study were presented at the Acoustical Society of America (ASA) meeting in November 2006 [3], the NPAL workshop in May 2007, the ASA meeting in June 2007 [4], the NPAL workshop in May 2008, and the ASA meeting in June-July 2008 [1].

LOAPEX Analysis: The low mode signals received during LOAPEX were processed. Mooring motion data was missing for some days of the LOAPEX experiment. A method was developed to estimate the missing data, and those corrections were applied to the receptions prior to mode processing. The interpolation method developed for the mooring data was presented at the MTS/IEEE Oceans Conference in September 2008 [2].

Kauai Analysis: The signals received during the 2004 NPAL experiment from the source deployed to the north of Kauai were processed and analyzed. Statistics of the low order modes, such as mean, variance, mean power, kurtosis, and skewness, were estimated. The results of this analysis were presented at the NPAL Workshop in April 2006.

RESULTS

This section discusses signal processing methods for estimating the mode travel times and the implementation of tomographic inversions using those travel times. The first part focuses on the use of matched subspace detectors for travel time estimation. The second part describes mode tomography using the LOAPEX data set.

Matched Subspace Detectors: This section considers the problem of mode travel time estimation for acoustic tomography. Assuming adiabatic propagation, the received time series for mode m at a range r can be written

$$a_m(t) = \beta \int S(\omega) \phi_m(\omega, z_{\text{src}}) \frac{e^{j(\omega t - \bar{k}_m r)}}{\sqrt{\bar{k}_m r}} d\omega,$$

where β is a constant, $S(\omega)$ is the source spectrum, $\phi_m(\omega, z_{\text{src}})$ is the modeshape at the source depth, and \bar{k}_m is the range-averaged mode wavenumber. A standard way to estimate the travel time of a known

signal is to implement a matched filter (MF) and use the peak of the MF output to determine the arrival time. There are several ways to design the MF, depending on what is assumed about the waveguide. The simplest way to design the MF for mode signals is to assume that the modeshape at the source depth is constant across the band of interest and that dispersion effects are negligible. In this case the received mode signal is a scaled version of the source signal $s(t)$ defined below:

$$s(t) = \beta \int S(\omega) e^{j\omega t} d\omega.$$

The MF for a signal $s(t)$ is the time-reversed version of the signal, *i.e.*, $h_{\text{MF}} = s(-t)$. For the remainder of this discussion, this version of the MF is called the standard MF.

Since the spectrum of the modeshape at the source depth is not always constant, it makes sense to extend the MF design to incorporate the effects of $\phi_m(\omega, z_{\text{src}})$. Assuming that the modeshapes are only a function of the known background (quiescent) sound speed profile and that dispersion effects are negligible, the received mode signal is

$$s_{\text{quiescent}}(t) = \beta \int S(\omega) \phi_m(\omega, z_{\text{src}}) e^{j\omega t} d\omega.$$

The matched filter that incorporates the scaling due to the quiescent spectrum of the modeshape at the source depth is $h_{\text{quiescent}} = s_{\text{quiescent}}(-t)$. The quiescent MF is most useful when the mode spectrum varies substantially across the band of the source, which typically happens when the source is located near a null in the mode.

The Matched Subspace Detector (MSD), proposed by Scharf and Friedlander [11], is an extension to the matched filtering concept that allows for received signals to be characterized by a known subspace, rather than requiring them to be described by a single vector. This project applied MSDs to the problem of detecting the arrival of mode signals affected by internal waves. Internal waves perturb the arrival time of the modes (by perturbing the mode wavenumbers) and perturb how the mode is excited by changing the modeshape $\phi_m(\omega, z_{\text{src}})$. Assuming that the modeshape perturbations are random, the second order statistics of the received mode signal can be used to define the subspace used in the MSD. For this project the eigenvectors of the correlation matrix for the internal-wave-perturbed mode signals were used to construct the subspace. Numerical simulations for the LOAPEX environment at 50 km range showed that the two eigenvectors associated with the two highest eigenvalues of the correlation matrix are sufficient to describe most of the mode energy. 1D and 2D MSDs were constructed for all the modes and used to estimate the mode travel times. Figures 1 and 2 show the output of the two matched filters and the 1D and 2D MSDs for modes 1 and 10 for two different simulated realizations of the internal wave field. For mode 1 the outputs of the four different types of filters are basically identical. The mode 1 spectrum is essentially flat across the source band, thus including the $\phi_m(\omega, z_{\text{src}})$ term does not have much effect. Any of the four filters can be used to determine the arrival time of mode 1; the arrival time is estimated as the time associated with the peak of the filter outputs. For mode 10, the results are significantly different. In this example, the source depth is near a null of mode 10, thus the mode excitation spectrum has a greater effect on what the received times series looks like. The location of the null changes with different internal wave realizations, and the shape of the received time series varies with each realization. The 2D MSD filter captures this variability, and the output of this filter contains a single peak located at the correct arrival time for both internal wave realizations. The standard and quiescent matched filters and the 1D MSD filter work well for one of the two realizations,

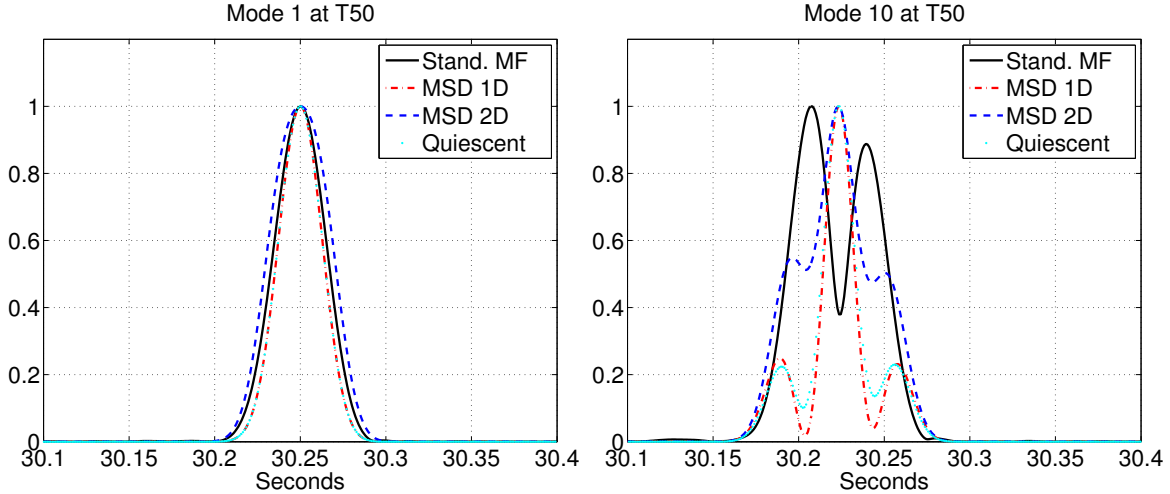


Figure 1: *Outputs of the standard MF, quiescent MF, and the 1D and 2D MSD processors for modes 1 and 10 of a simulation at 50 km. The plots show the results for one realization of the internal wave field. For mode 1 the four filters produce similar results and any of the filters could be used to estimate the mode 1 arrival time. For mode 10, the 2D MSD and quiescent MF could be used to estimate arrival time since they each produce an output with a single peak at the correct time. The standard MF and 1D MSD processors have outputs with multiple peaks, making time of arrival estimation substantially more difficult.*

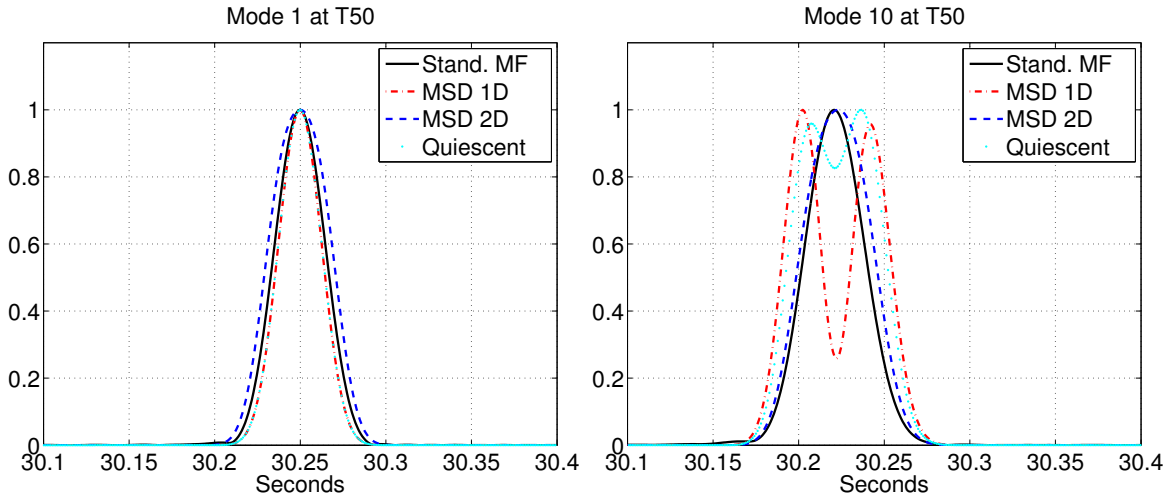


Figure 2: *Outputs of the standard MF, quiescent MF, and the 1D and 2D MSD processors for modes 1 and 10 of a simulation at 50 km. The plots show the results for a different realization of the internal wave field than Figure 1. For mode 1 the four filters produce similar results and any of the filters could be used to estimate the mode 1 arrival time. For mode 10, the 2D MSD and the standard MF could be used to estimate arrival time since they each produce an output with a single peak at the correct time. The quiescent MF and 1D MSD processors have outputs with multiple peaks, making time of arrival estimation substantially more difficult.*

but not for the other. These plots demonstrate the effectiveness of the 2D MSD filter for estimating the arrival times of modes in this environment.

Consider the results of travel time estimation using the standard MF and the 1D and 2D MSD processors for the LOAPEX data set. Figure 3 shows the travel time estimates for station T50 produced using the four filters. The plot compares the travel time estimates with the travel times predicted by the sound speed profiles measured at the receiving array and the source location (approximately 50 km from the receiver). For modes 6, 7, 9 and 10, which have nulls in their excitation spectra at the source depth, the 1D MSD and standard MF have significantly larger travel time variance than the 2D MSD, as expected. The travel time estimates of all three methods are closer to the predictions for the Seabird profile (measured at the array) than to the CTD profile measured at the source. Figure 4 shows the travel time estimates for station T250. At this range, there is not much difference between the estimates provided by the three different methods.

At 500 km, the number of eigenvectors required to represent most of the energy in modes 1 to 10 is significantly greater than the number required at T50. Simulations at 500 km showed that MSDs of dimensions ranging from 4 to 9 were required to describe most of the energy in modes 1 to 10. Figure 5 shows the travel time estimates obtained using the MSDs for the first 10 modes at 500 km. The MSD estimates are compared with those obtained by picking the peaks of the output of a standard matched filter. The left plot shows the mean of the travel time estimates, and the right plot shows the standard deviation of the estimates. The MSD travel time estimates are similar to the travel time predictions of the background profile. The peak-picking approach has a high standard deviation on the order of 40-50 ms. Most of the travel time variance of peak picking is due to the significant amount of internal-wave-induced multipath. The MSD on the other hand has a much smaller travel time standard deviation on the order of 10-15 ms. The standard deviation of the MSD is primarily due to travel time wander due to internal waves variations and not due to errors associated with scattering. Based on the travel time simulation examples and travel time estimation statistics such as those presented in this section, MSDs are flexible enough to accommodate the different types of internal wave scattering for each mode and the different ranges.

Mode Tomography: This section describes the implementation of mode tomography for the LOAPEX environment and then discusses the results of the inversion. The inverse implemented for LOAPEX used the perturbation theory approach of Munk and Wunsch [9], where perturbations in mode travel time are inverted for perturbations in sound speed. Based on previous work [7, 8, 12, 10], it is assumed that the sound speed perturbations can be characterized by a small set of depth-dependent basis functions. For LOAPEX the basis consisted of a set of empirical orthogonal functions (EOF's) derived from environmental data recorded on the vertical line array used in the experiment. The time-averaged SSP at the array was used as the reference profile, and the EOF's were computed from an eigendecomposition of the correlation matrix of the recorded perturbations about the reference profile. The input to the inversion was the mode travel time perturbations, obtained by subtracting the mode travel times for the reference profile from the mode travel times measured using the methods described in the previous section.

Figure 6 shows the results of the tomographic inversion at 50 km range (LOAPEX station T50), obtained using the three types of travel time estimates shown in Figure 3. Each plot in the figure compares the estimated sound speed perturbation with the perturbation associated with the CTD measurement at the T50 source location and the Seabird measurement at the receiver location. Since the 2D MSD method produces travel time estimates with lower variance, it is not surprising that the

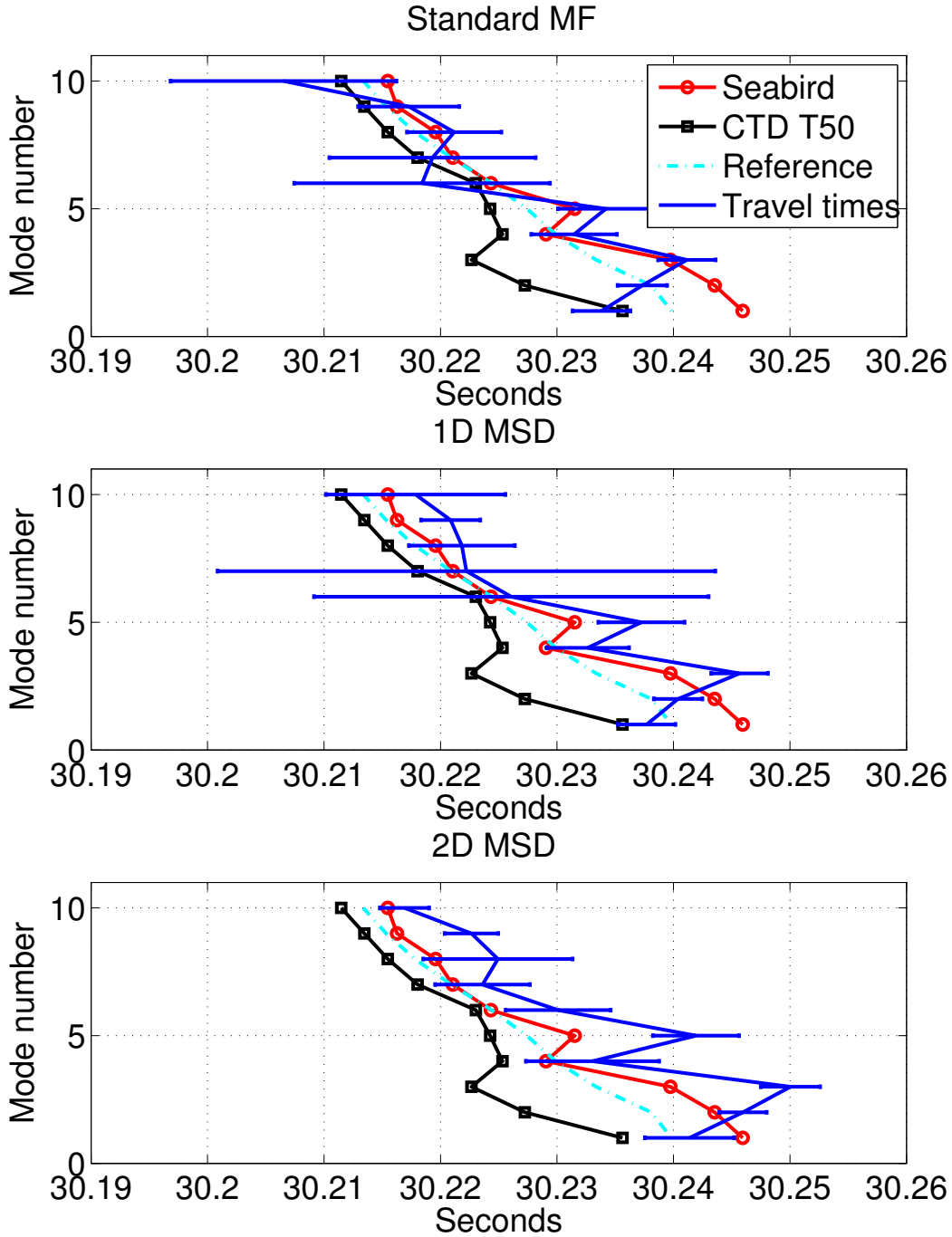


Figure 3: Travel time estimates at LOAPEX station T50 using the standard MF and the 1D and 2D MSD processors. The errorbars indicate the standard deviation of the estimates. Predicted travel times are shown for two measured sound speed profiles and a background reference profile. The prediction denoted Seabird is the for the profile measured at the receiving array and the prediction denoted CTD T50 is for the profile measured at the source. The travel time estimates are closer to the Seabird profile than the source profile. The 2D MSD has a lower travel time variance than the other two methods.

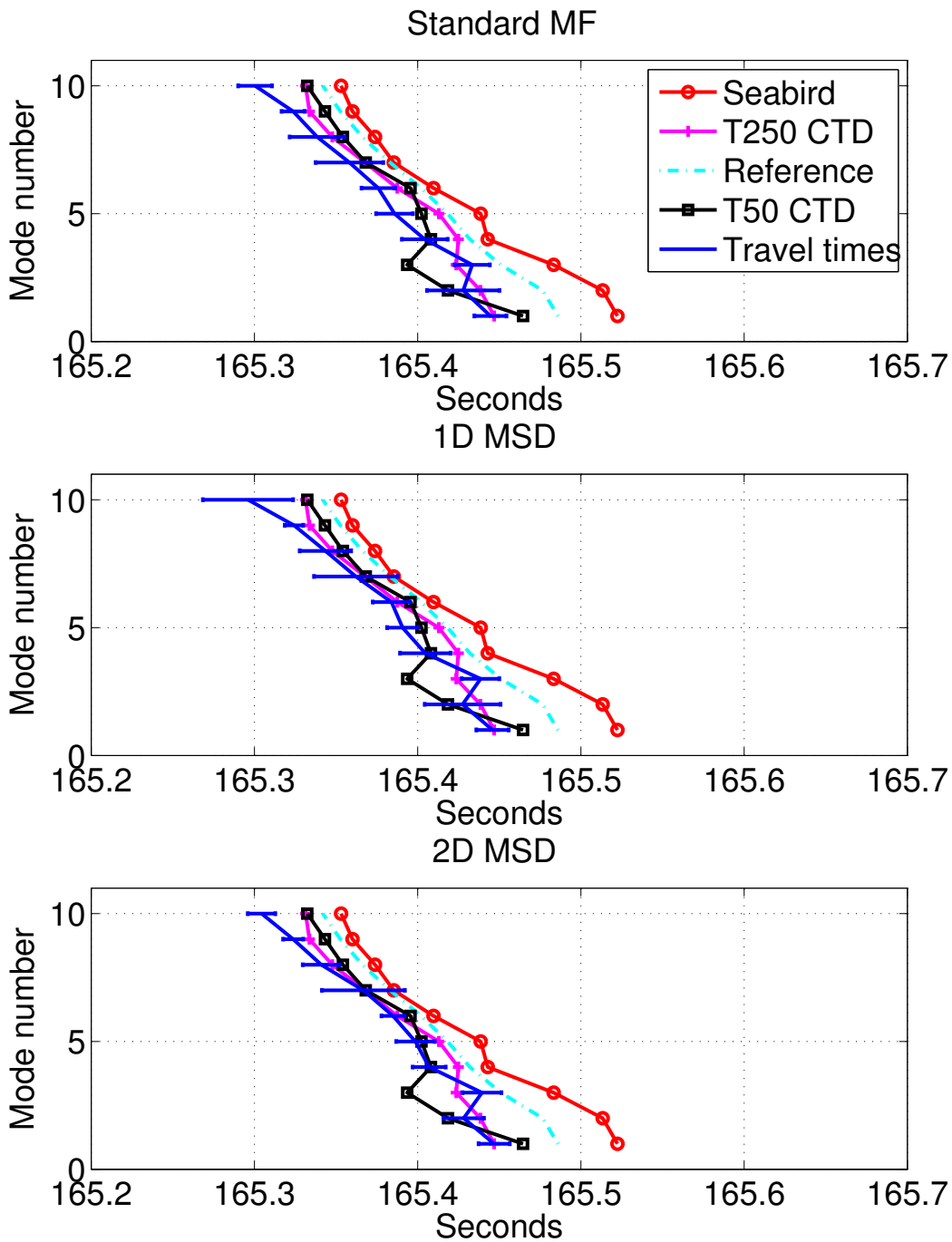


Figure 4: Travel time estimates at LOAPEX station T250. Errorbars indicate the standard deviation of the estimates. Predictions are shown for three measured profiles: the Seabird profile measured at the receiving array, and the CTD profiles measured at stations T50 and T250. The estimates for the three methods all lie close to the travel times predicted by the measured sound speed profiles at T50 and T250. Similar to the results for T50, the MSD travel times have a lower variance than the standard MF estimates.

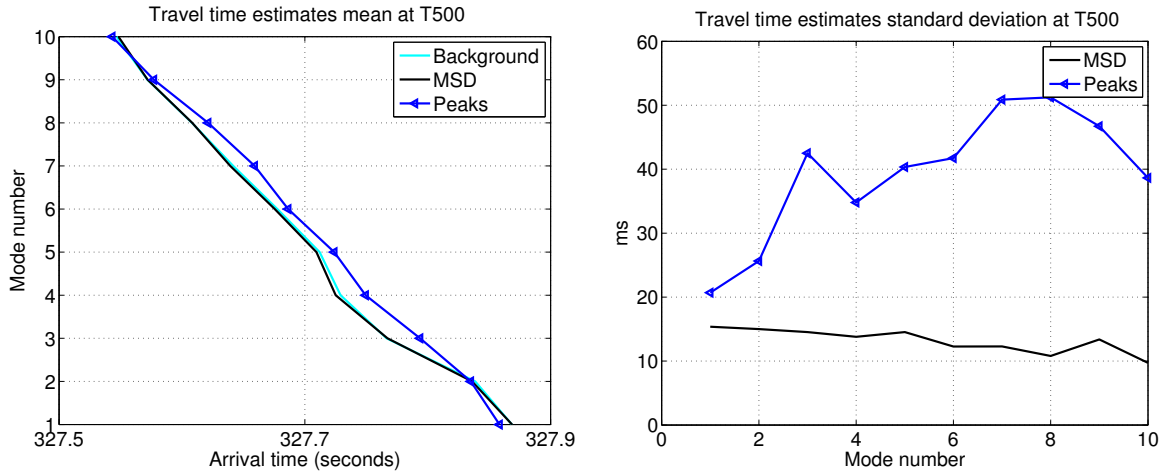


Figure 5: Mean (left plot) and standard deviation (right plot) of travel time estimates at 500 km from simulations. The MSD travel time estimates have a mean that is close to the travel time estimates of the background SSP. The standard deviations of the MSD travel time estimates are much smaller than the standard deviations of the peak-picking results.

inverted profile obtained from the 2D MSD processor has lower variance than the 1D MSD and standard MF processors. Note that there is a significant difference in the sound speed at the source (CTD profile) and the sound speed at the receiver (Seabird profile). The inverted profile is closer to the receiver measurement than to the source measurement, suggesting that the recorded modes propagated primarily in an environment resembling that at the receiver. Figure 7 shows the results of the inversion at 250 km range (station T250) obtained using the travel time measurements shown in Figure 4. Similar to T50, the 2D-MSD result at T250 shows significantly lower variance than the other two methods. At 250 km range, the inverted profile lies between the CTD measurements obtained at stations T50 and T250, though it is closer to the T250 measurement. Figure 8 shows the inversion results for a range of 500 km (station T500). Figure 8 compares the inverted result with the Seabird measurement at the receiver, CTD measurements at three LOAPEX stations, and the average of the Seabird profile and the three CTD profiles. The inverted result at T500 is closest to the average profile, which makes sense since the modes effectively propagate through the range-averaged environment.

In summary, this project has successfully implemented mode tomography for ranges up to 500 km. The inverted sound speed profiles show good agreement with environmental measurements. At ranges up to 500 km, the MSD approach for estimating travel times provides a significant reduction in variance of the estimates.

IMPACT/APPLICATIONS

This research has signal processing and scientific applications. First, this work has demonstrated that subspace processing methods can substantially improve detection and estimation in an environment affected by internal waves. Second, this project has demonstrated the feasibility of mode tomography at ranges up to 500 km. Since the low modes are concentrated around the sound channel axis, mode-based tomography should enhance the sound speed resolution at axial depths.

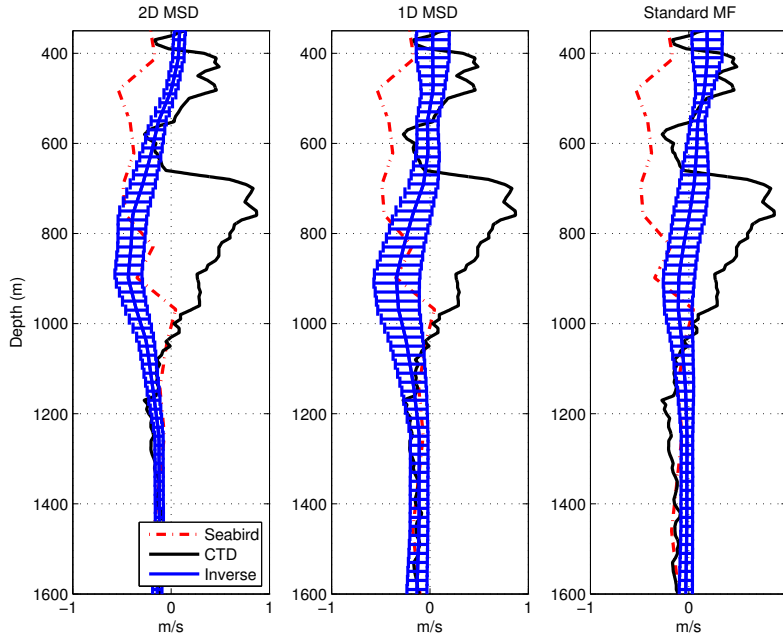


Figure 6: *Inverted sound speed perturbations at LOAPEX station T50. The inverted sound speeds are close to those associated with the Seabird measurement made at the receiving array. The errorbars show that the 2D MSD processor has lower variance than the other two processors.*

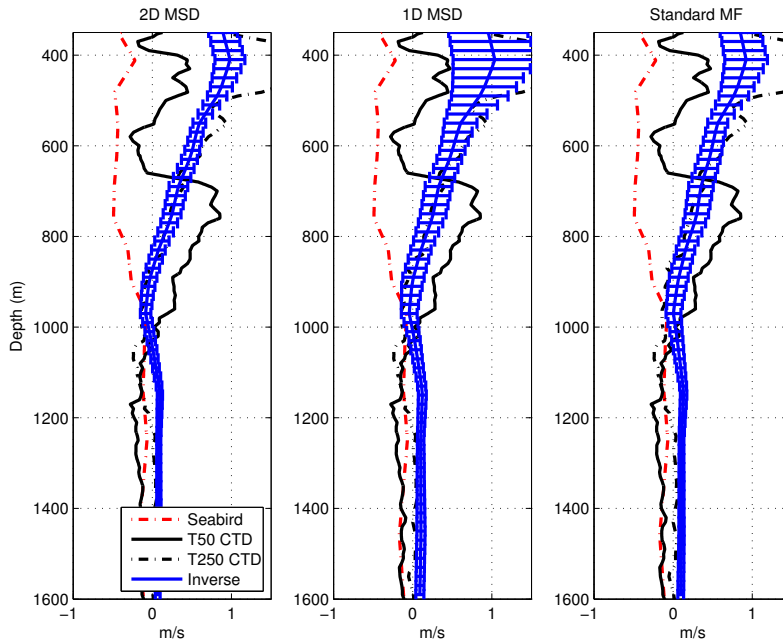


Figure 7: *Inverted sound speed perturbations at LOAPEX station T250. The inversion results are close to the CTD measurement at T250. The errorbars show that the 2D MSD processor leads to a lower variance in the inversion results.*

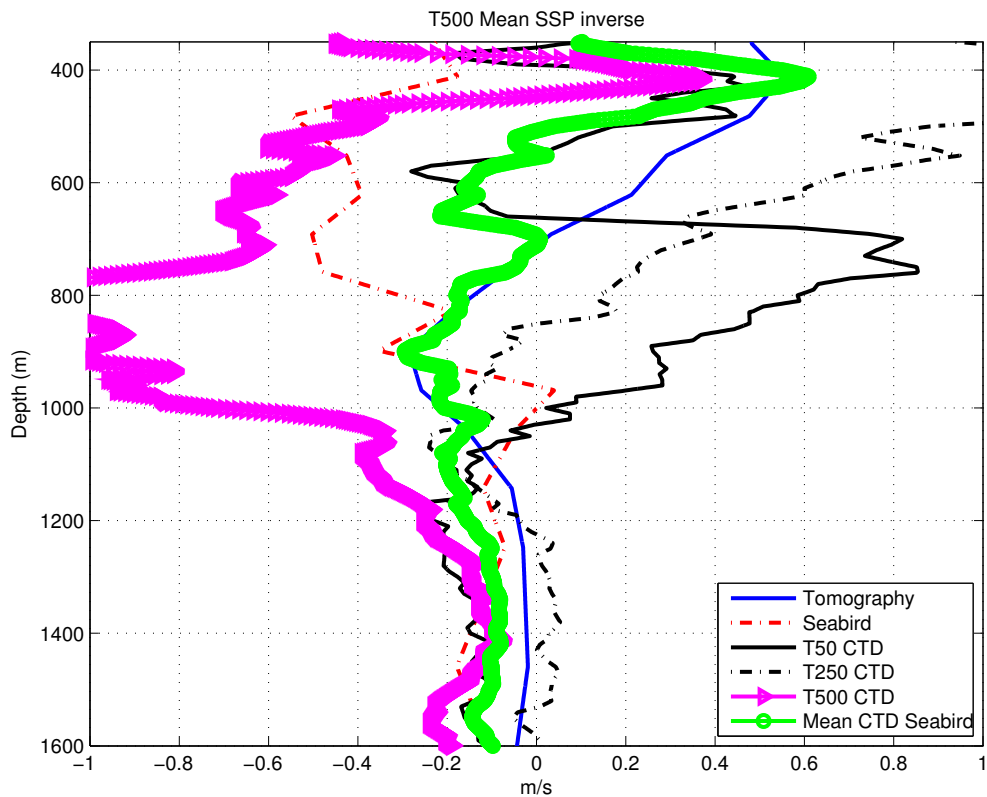


Figure 8: *Inverted sound speed perturbations at LOAPEX station T500 obtained using the standard MF travel time estimates for modes 1 to 10. The mean of the sound speed inverse is close to the average SSP obtained by averaging the measured profiles across the T500 path.*

RELATED PROJECTS

This work is closely related to ONR Award N00014-09-1-0675, which is the grant funding Dr. Chandrayadula's advisor Kathleen Wage. It is also related to the work being done by the North Pacific Acoustic Laboratory group coordinated by principal investigators Peter Worcester (Scripps) and James Mercer (APL - UW). Many other ONR-sponsored researchers work on projects related to NPAL and participate in the NPAL workshops.

REFERENCES

- [1] T. K. Chandrayadula and K. E. Wage. Evolution of the statistics of the unscattered component of low order acoustic modes as a function of range. *J. Acoust. Soc. Am*, 123(5):3463, 2008.
- [2] T. K. Chandrayadula and K. E. Wage. Interpolation methods for vertical linear array element localization. In *Proceedings of the MTS/IEEE Oceans 2008 Conference*, Quebec, Canada, September 2008.
- [3] T. K. Chandrayadula, K. E. Wage, J. A. Mercer, B. M. Howe, R. K. Andrew, P. F. Worcester, and M. A. Dzieciuch. Evolution of second-order statistics of low-order acoustic modes. *J. Acoust. Soc. Am*, 120(5):3062, 2006.
- [4] T. K. Chandrayadula, K. E. Wage, J. A. Mercer, B. M. Howe, R. K. Andrew, P. F. Worcester, and M. Dzieciuch. Signal processing techniques for low-order acoustic modes. *J. Acoust. Soc. Am.*, 121(5):3053, 2007.
- [5] T. K. Chandrayadula, K. E. Wage, J. A. Mercer, B. M. Howe, R. K. Andrew, P. F. Worcester, and M. A. Dzieciuch. Robust observables for mode tomography. *J. Acoust. Soc. Am*, 126(4):2172, 2009.
- [6] J. A. Colosi and M. G. Brown. Efficient numerical simulation of stochastic internal-wave-induced sound-speed perturbation fields. *J. Acoust. Soc. Am.*, 103(4):2232–2235, April 1998.
- [7] B. D. Cornuelle. *Inverse Methods and Results from the 1981 Ocean Acoustic Tomography Experiment*. PhD thesis, MIT, 1983.
- [8] B. M. Howe, P. F. Worcester, and R. C. Spindel. Ocean acoustic tomography: Mesoscale velocity. *Journal of Geophysical Research*, 92(C4):3785–3805, April 1987.
- [9] W. Munk and C. Wunsch. Ocean acoustic tomography : Rays and modes. *Reviews of Geophysics and Space Physics*, 21:777–793, 1983.
- [10] J. J. Romm. *Applications of Normal Mode Analysis to Ocean Acoustic Tomography*. PhD thesis, MIT, 1987.
- [11] L. L. Scharf and B. Friedlander. Matched subspace detectors. *IEEE Transactions on Signal Processing*, pages 2146–2157, August 1994.
- [12] P. Sutton, W. Morawitz, B. Cornuelle, G. Masters, and P. Worcester. Incorporation of acoustic normal mode data into tomographic inversions in the Greenland Sea. *Journal of Physical Oceanography*, 99:12487–12502, June 1994.

PUBLICATIONS

Tarun K. Chandrayadula and Kathleen E. Wage, "Interpolation methods for vertical linear array element localization" in *Proceedings of the MTS/IEEE Oceans 2008 Conference*, Quebec, Canada, pp. 1-5, September 2008. [published]

Tarun K. Chandrayadula, *Mode Tomography Using Signals from the Long Range Acoustic Propagation Experiment (LOAPEX)*, PhD thesis, George Mason University, 2010.

HONORS/AWARDS/PRIZES

Dr. Tarun K. Chandrayadula received a National Research Council Research Associateship Award in April 2010. This award is funding his post-doctoral research at the Naval Postgraduate School.